

Geostatistical AVO inversion on a deepwater oil field

Pål Dahle, Ragnar Hauge, and Odd Kolbjørnsen
Norwegian computing Center,

Ernesto Della Rossa, Fabio Luoni, and Alfonso Junio Marini,
ENI

SUMMARY

Seismic inversion is usually treated as a deterministic problem. However, since the seismic amplitude data contains noise and the frequency resolution is limited, high and low frequencies will be uncertain. For a consistent treatment of these uncertainties, a geostatistical inversion method can be used.

We have used a Bayesian linearised AVO inversion method for a turbiditic channel system reservoir containing two offset stacks. In this Bayesian approach, the earth model parameters V_p , V_s , and ρ are given by a multi-normal distribution where spatial coupling is imposed by correlation functions. A linearised relationship between the model parameters and the AVO data, allows us to obtain the posterior distribution for the earth model parameters analytically.

The posterior distribution represents a laterally consistent seismic inversion where the solution in each location depends on the solutions in all other locations. The distribution contains the best estimate of the model parameters as well as their associated uncertainties. Using kriging, full frequency information from well data are spread in a volume around the wells; and from the posterior uncertainty, we generate full frequency solutions for the entire volume.

The Bayesian approach is fast and the inversion gave good match with well log data.

INTRODUCTION

Seismic inversion has traditionally been treated as a deterministic problem. However, there are several uncertain aspects. There is noise in the seismic amplitude data, and the frequency resolution is limited so neither high nor low frequencies can be resolved from the seismic data alone. Using a geostatistical approach to the problem of seismic inversion, the uncertainty may be treated in a consistent and robust way. We have used the Bayesian linearised AVO inversion method of Buland et al. (2003) to take the uncertainty in seismic data into account. In this method, the logarithm of the earth model parameters V_p , V_s , and ρ defines a multi-normal distribution in which spatial coupling is imposed by correlation functions. A linearised relationship between the model parameters and the AVO data, allows us to obtain the posterior distribution for the earth model parameters analytically.

The posterior distribution represents a laterally consistent seismic inversion. The lateral correlation follows the stratigraphy of the reservoir by following the top and base of the inversion volume. As a consequence of the spatial coupling, the solution in each location depends on the solutions in all other locations. From the posterior distribution the best estimate of the model parameters and a corresponding uncertainty can be extracted. Also, since the distribution is multi-normal, kriging can be used to match the well data. This spreads full frequency information in a volume around the wells. Full frequency solutions can be generated by sampling from the posterior distribution. A set of such solutions represents the uncertainty of the inversion.

We have applied this approach to a turbiditic channel system located in a deepwater reservoir. Two seismic volumes having 15 and 40 degrees offset stacks were used for the inversion. Both volumes were sampled every 4ms.

THEORY

An isotropic, elastic medium is completely described by three material parameters $\{V_p(\mathbf{x}, t), V_s(\mathbf{x}, t), \rho(\mathbf{x}, t)\}$, where V_p is the P-wave velocity, V_s is the S-wave velocity, and ρ is the density. The elastic parameters depend on the lateral position \mathbf{x} and on the vertical seismic travel time t . If we model the elastic parameters as log-Gaussian random fields, the vector field $\mathbf{m}(\mathbf{x}, t) = [\ln V_p(\mathbf{x}, t), \ln V_s(\mathbf{x}, t), \ln \rho(\mathbf{x}, t)]$, becomes Gaussian. That is

$$(1) \quad \mathbf{m}(\mathbf{x}, t) = N(\boldsymbol{\mu}_m(\mathbf{x}, t), \Sigma_m),$$

where $\boldsymbol{\mu}_m(\mathbf{x}, t)$ contains the expectations of the logarithm of the elastic parameters for all \mathbf{x} and t , and Σ_m defines the covariance structure. The covariance function is assumed to be translationally invariant (i.e. stationary and homogeneous).

If we use a weak contrast approximation to the seismic reflectivity function $c(\mathbf{x}, t, \theta)$ (see Stolt and Weglein (1985)), and use a constant value for the ratio V_p/V_s in the expressions, we get a linear relationship between the elastic parameters and the reflectivity function. Moreover, if we let the seismic data be represented by a convolutional model, and model the data as the seismic response of the earth model plus an error term, where the error is assumed zero mean coloured Gaussian noise, the seismic data \mathbf{d}_{obs} are also multi-normal.

In a Bayesian setting, prior models for the earth and error terms are set up based on prior knowledge obtained from well logs, and the seismic inversion is equivalent to finding a posterior distribution for the earth given the seismic data. The linear relationship between the earth model parameters and seismic data implies that the simultaneous distribution for \mathbf{m} and \mathbf{d}_{obs} is also multi-normal. The posterior distribution, that is, the distribution for \mathbf{m} given \mathbf{d}_{obs} can therefore be obtained using standard theory:

$$(2) \quad \boldsymbol{\mu}_{m|\mathbf{d}_{\text{obs}}} = \boldsymbol{\mu}_m + \Sigma_{d,m}^T \Sigma_d^{-1} (\mathbf{d}_{\text{obs}} - \boldsymbol{\mu}_d),$$

$$(3) \quad \Sigma_{m|\mathbf{d}_{\text{obs}}} = \Sigma_m - \Sigma_{d,m}^T \Sigma_d^{-1} \Sigma_{d,m},$$

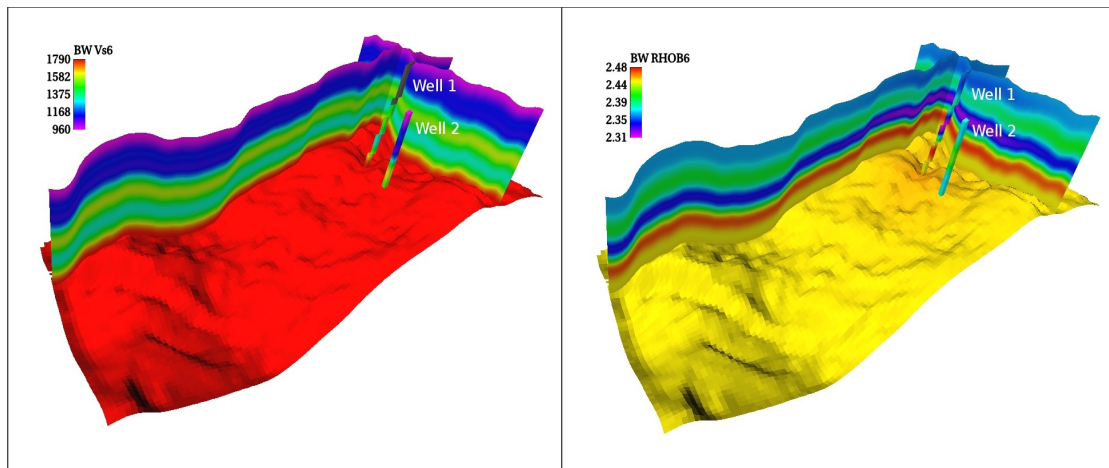


Figure 1: Cross sections of the background model volumes for V_s and ρ . In the prior model, the natural logarithms of these volumes are used. The background model for V_p is similar to that of V_s .

where μ_d is the expected observation, that is, the seismic response of μ_m , and $\Sigma_{d,m}$ is the covariance matrix between logarithmic parameters and observations. For more details on how to compute these, see Buland et al. (2003).

The computations given in equations (2) and (3) involves the inverse of Σ^{-1}_d . Given n_θ offset stacks and inversion volumes with n cells, this matrix has $n_\theta^2 n^2$ elements, making a direct inversion impossible for real cases. However, the covariance function for a homogeneously correlated spatial variable is diagonalised by a 3D Fourier transform (see Christakos (1992)), allowing the inversion problem to be solved independently for each frequency component. This reduces the complexity of the computations dramatically, and the calculation time becomes $O(n \log n)$. Details can again be found in Buland et al. (2003).

DEEPWATER RESERVOIR CASE

The prior model for the Bayesian inversion consists of the expectation value μ_m and the spatial correlation Σ_m . Both of these must be assigned values before the inversion.

The expectation μ_m is the background model for the inversion, and is needed to set the appropriate levels for V_p , V_s , and ρ in the inversion volume. As seen in equation (2), the signal response of the background, μ_d , is subtracted from the seismic data in the inversion process, and after the inversion, the background is added. To generate the background model, low frequencies were extracted from well logs for V_p , V_s , and ρ by filtering raw logs to 6 Hz. These filtered logs were aligned according to stratigraphic depth, and an arithmetic mean was estimated for each elastic parameter. This mean was used as a global depth trend throughout the volume. To also account for local information contained in wells, the difference between the 6 Hz log and the global trend was interpolated into the volume using kriging. In Figure 1 we have shown cross sections of the final background volumes.

The parameter variances and covariances and the temporal correlation which constitute parts of the covariance matrix Σ_m , were estimated directly from well data, while a parametric correlation functions with ranges 1500m and 500m were used for the lateral correlation. This lateral correlation was also used in the error model, while the temporal error correlation was partly computed from the wavelet and partly white noise. The noise at 40 degrees was assumed to be uncorrelated with the noise at 15 degrees.

INVERSION RESULTS

The inversion interval was set to include 100ms over and under the structure depicted in Figure 3. The inversion was run with a 25m×25m lateral resolution and a sampling density of

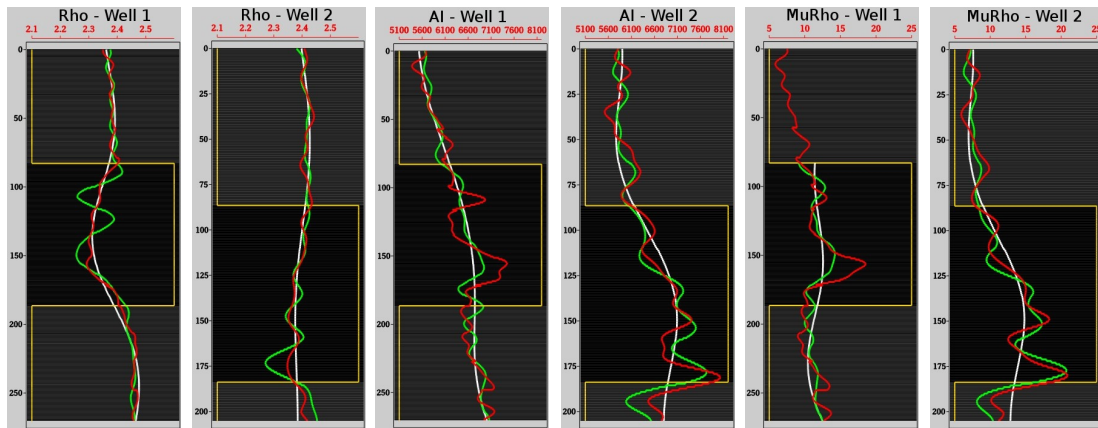


Figure 2: Well logs showing density, acoustic impedance, and $\mu\rho$ for the two wells. Each well log shows a 6 Hz high cut filtered well log (white), a 40 Hz high cut filtered well log (green), and the inversion (red). Also outlined is the interval of reservoir interest (orange).

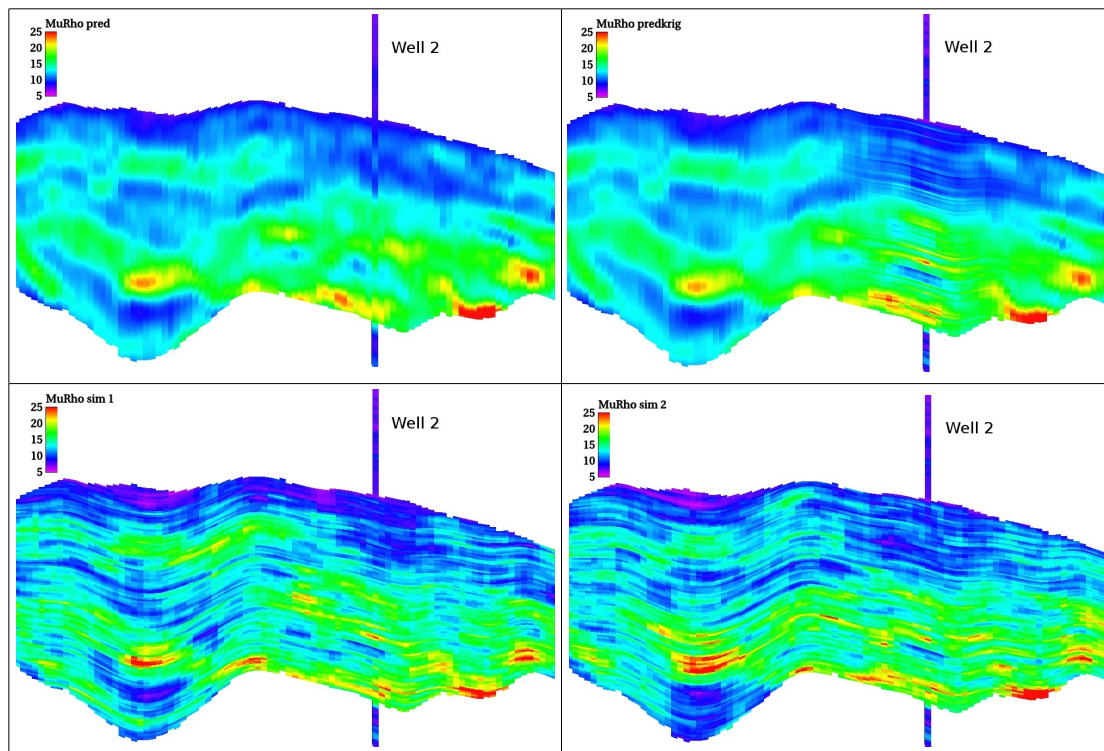


Figure 3: Cross sections which pass through well 2 and show predicted and simulated $\mu\rho$.

1ms. This resulted in a $446 \times 221 \times 300$ grid containing some 30,000,000 grid cells. Using a standard 64 bits Linux PC, a simulation run conditioned to wells completed in 15 minutes.

In Figure 2, we show well logs for the two wells and the inversion results. Since well 1 is deviating, the best estimates are obtained in well 2. Moreover, the parameter estimated best is the $\mu\rho$, but the acoustic impedance (AI) is also fairly good. For the density the deviations from the background model is too small. This is possibly because the density contrast has much less variability than V_p and V_s , hence most of the variability in the reflection coefficients is explained by the latter contrasts. The $\mu\rho$ was later used for facies modelling.

In Figure 3, four different inversion results are presented: predicted $\mu\rho$ (top left), predicted $\mu\rho$ conditioned to well data (top right) and two different simulations of $\mu\rho$ also conditioned to well data. For the prediction we have plotted the 40 Hz filtered well data for comparison. The cross section shows good match between predicted $\mu\rho$ and well log data. The prediction is frequency limited with the maximum frequency of around 40-50 Hz, while the simulations

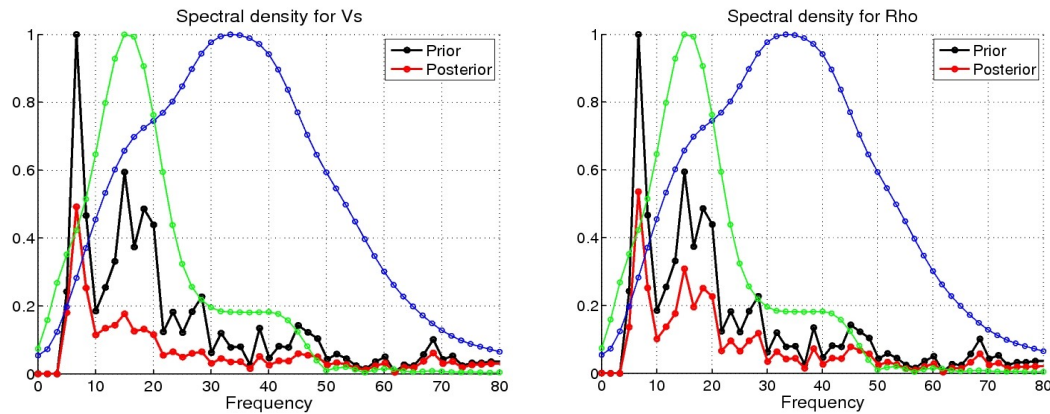


Figure 4: Uncertainties (spectral densities) for V_s (left) and Rho (right) for each frequency. The prior uncertainty is shown as black and the posterior uncertainty as red. Also shown are the spectral densities of the near wavelet (blue) and the far wavelet (green).

shown in Figures 3 contain the same frequency range as the well logs.

In addition to updating the expected values for the elastic parameters, the inversion also reduces the uncertainty, as seen in equation (3). The variance is reduced by 45%, 35%, and 5% for the parameters V_p , V_s , and ρ respectively. The largest reduction is for frequencies between 5Hz and 55Hz, consistent with the frequency content of the seismic data. The uncertainty reduction for each frequency is illustrated by the spectral densities (the Fourier transform of the temporal correlation) shown in Figure 4.

CONCLUSIONS

The inversion approach used for this case study has the following main advantages:

- 1) The method is fast compared with traditional inversions.
- 2) Spatial coupling both in parameters and noise is handled correctly. Spatial correlation between traces creates realistic spatial continuity.
- 3) In addition to the prediction (expected value), simulations conditioned to well logs are generated. This gives an uncertainty assessment in the inversion parameters.
- 4) It is possible to use stochastic simulation to create realizations of high-resolution seismic inversions by drawing from the posterior probability distribution.

Four assumptions are made, two of which are common: The weak contrast approximation and the convolution model. In addition, the elastic parameters are assumed log-Gaussian fields, second-order stationary around the background model. Finally, it is also assumed that the seismic residuals are second-order stationary Gaussian fields. The stationarity is needed to achieve the diagonalisation through the Fourier transform, and is the most limiting aspect of the approach. For the current case, the stationarity assumptions seems to be justified.

ACKNOWLEDGMENT

We thank ENI for permission to publish this paper.

REFERENCES

- Buland, A., Kolbjørnsen, O., and Omre, H. [2003] Rapid spatially coupled AVO inversion in the fourier domain, *Geophysics* 68, 824-836.
- Christakos, G. [1992] *Random field models in earth sciences*, Academic Press Inc., San Diego
- Stolt, R., H., and Weglein, A., B. [1985] Migration and inversion of seismic data, *Geophysics* 50, 2458-2472.